Formation of Novel Dinuclear Lanthanide Luminescent Samarium(III), Europium(III), and Terbium(III) Triple-Stranded Helicates from a C_2-Symmetrical Pyridine-2,6-dicarboxamide-Based 1,3-Xylenediyl-Linked Ligand in MeCN

by **Steve Comby**[a]), **Floriana Stomeo**[a]), **Colin P. McCoy**[b]), and **Thorfinnur Gunnlaugsson***[a])

[a]) School of Chemistry, Centre for Synthesis and Chemical Biology, Trinity College Dublin, IE-Dublin 2 (phone: +353 1 8963459; fax: +353 1 671 2826; e-mail: gunnlaut@tcd.ie)

[b]) School of Pharmacy, Queen's University of Belfast, 97 Lisburn Road, UK-Belfast, BT9 7BL

Dedicated to Professor *Jean-Claude Bünzli* on the occasion of his 65th birthday

The synthesis of the C_2-symmetrical ligand **1** consisting of two naphthalene units connected to two pyridine-2,6-dicarboxamide moieties linked by a xylene spacer and the formation of Ln^{III}-based (Ln = Sm, Eu, Tb, and Lu) dimetallic helicates $[Ln_2 \cdot \mathbf{1}_3]$ in MeCN by means of a metal-directed synthesis is described. By analyzing the metal-induced changes in the absorption and the fluorescence of **1**, the formation of the helicates, and the presence of a second species $[Ln_2 \cdot \mathbf{1}_2]$ was confirmed by nonlinear-regression analysis. While significant changes were observed in the photophysical properties of **1**, the most dramatic changes were observed in the metal-centred lanthanide emissions, upon excitation of the naphthalene antennae. From the changes in the lanthanide emission, we were able to demonstrate that these helicates were formed in high yields (*ca.* 90% after the addition of 0.6 equiv. of Ln^{III}), with high binding constants, which matched well with that determined from the changes in the absorption spectra. The formation of the Lu^{III} helicate, $[Lu_2 \cdot \mathbf{1}_3]$, was also investigated for comparison purposes, as we were unable to obtain accurate binding constants from the changes in the fluorescence emission upon formation of $[Sm_2 \cdot \mathbf{1}_3]$, $[Eu_2 \cdot \mathbf{1}_3]$, and $[Tb_2 \cdot \mathbf{1}_3]$.

Introduction. – The use of metal-directed synthesis in the construction of complexed supramolecular structures has recently become a very active research area [1–4]. To date, such structures have been mostly developed by using various transition-metal ions and organic ligands possessing defined coordination motives that match or complement the coordination requirements of the given transition-metal ion [5–7]. This strategy has resulted in the formation of many elegant examples of complex supramolecular structures, some of which possess the inherent physical properties of the coordinating ligands, in addition to those associated with the d-metal ions alone [8][9]. In contrast, the use of the lanthanide-metal ions in such supramolecular synthesis has been much less investigated [10–12]. However, as many of these ions possess both unique photophysical and magnetic properties, their use in metal-directed synthesis has grown, resulting in the publication of some elegant examples, notably in the area of lanthanide-directed helicate synthesis [13][14], as well as in the formation of lanthanide complexes possessing high symmetry [15]. This work has, in particular, been spearheaded by the pioneering work of *Bünzli* [2][16], who has developed varieties of examples of lanthanide-based helicates, and mixed f-d-metal-ion-based

helicates (some in collaboration with the group of *Piguet*), and studied their photophysical properties in solution and in the solid state [17][18]. Inspired by this work, we have recently embarked on the developments of functional lanthanide and mixed f-d-metal-ions self-assembly [19–22], as well as on using the f-metal ions for the formation of chiral luminescent self-assemblies, or 'coordination bundles' (sliotars), that possess a high degree of symmetry and display strong lanthanide luminescence upon excitation of the ligand antennae [23]. In this article, we present some recent results of our investigation into the development of novel structurally 'simple' C_2-symmetry-based bis[pyridine-2,6-dicarboxamide] ligands, such as **1**, possessing two chiral naphthalene moieties connected to two pyridine-2,6-dicarboxamide 'wings' linked by a 1,3-xylene spacer, that can be employed in the synthesis of dinuclear lanthanide-based helicates [24]. The formation of the three dimetallic triple-stranded helicates $[Sm_2 \cdot \mathbf{1}_3]$, $[Eu_2 \cdot \mathbf{1}_3]$, and $[Tb_2 \cdot \mathbf{1}_3]$ from **1** was analysed in MeCN solution by carrying out various spectroscopic titrations where the changes in the absorption and the fluorescence emission of **1** was monitored as well as the evolution of their respective lanthanide-centred emissions. For comparison, we also studied the formation of $[Lu_2 \cdot \mathbf{1}_3]$ in solution; however, unlike those above, this helicate does not give rise to metal-centred luminescence. Our results clearly show that all these lanthanide ions form helicates in MeCN solution, and that $[Sm_2 \cdot \mathbf{1}_3]$, $[Eu_2 \cdot \mathbf{1}_3]$, and $[Tb_2 \cdot \mathbf{1}_3]$ all give rise to characteristic sensitized lanthanide emissions upon excitation of the naphthalene antenna. We also demonstrate by fitting the various spectroscopic changes observed, by means of nonlinear regression analysis, that the desired metal/ligand 2:3 stoichiometry is the dominant species in solution for all of these helicates, the formation of dinuclear species, *e.g.*, $[Ln_2 \cdot \mathbf{1}_2]$, only occurring at higher ion concentrations.

Results and Discussion. – 1. *Synthesis of Ligand* **1**. The synthesis of **1** was achieved in a few steps starting from the commercially available pyridine-2,6-dicarboxylic acid, by first forming the corresponding pyridine-2,6-dicarboxylic acid monobenzyl ester [25] which was then treated with (1*S*)-1-(1-naphthyl)ethylamine in anhydrous THF, in the presence of HOBt, EDCI·HCl, and Et_3N (*Scheme*). This gave **2** in 81% yield after aqueous acid/base workup. Ester hydrolysis of **2** to give **3** was achieved in 98% yield in EtOH with 10% Pd/C catalyst (10% loading) under 3 atm pressure of H_2. Compound **3** was then subjected to the same peptide coupling reaction as employed for **2**, which gave the desired product **1** after workup in 25% yield as an off-white solid (see *Exper. Part*). Compound **1** was characterized by conventional methods (see *Exper. Part*). The high-resolution ESI-MS showed the presence of a species at *m*/*z* 763, which matched the calculated isotopic distribution pattern for $[M + Na]^+$, while the ^{1}H-NMR (600 MHz, $CDCl_3$; *Fig. 1*) clearly demonstrated the presence of a single species with C_2 symmetry, where the N–H resonances appeared as *d* at δ 8.70 and 8.53–8.44, respectively, and the H-atoms in α-position at δ 4.20 and 3.72 as a *dd*. The structure was fully assigned by means of ^{1}H,^{1}H-, ^{13}C,^{1}H-, and ^{14}N,^{1}H-COSY NMR experiments (see *Exper. Part*).

2. *Absorption and Fluorescence Spectroscopic Investigation of* **1** *in the Presence of Lanthanide Ions.* The absorption and the fluorescence-emission spectra of **1** were first recorded in MeCN solution. The absorption spectra consisted of two main bands, a high energy one at λ 223 nm and a longer-wavelength band with λ_{max} at 281 nm ($\varepsilon =$

Scheme. *Synthesis of Ligand* **1**

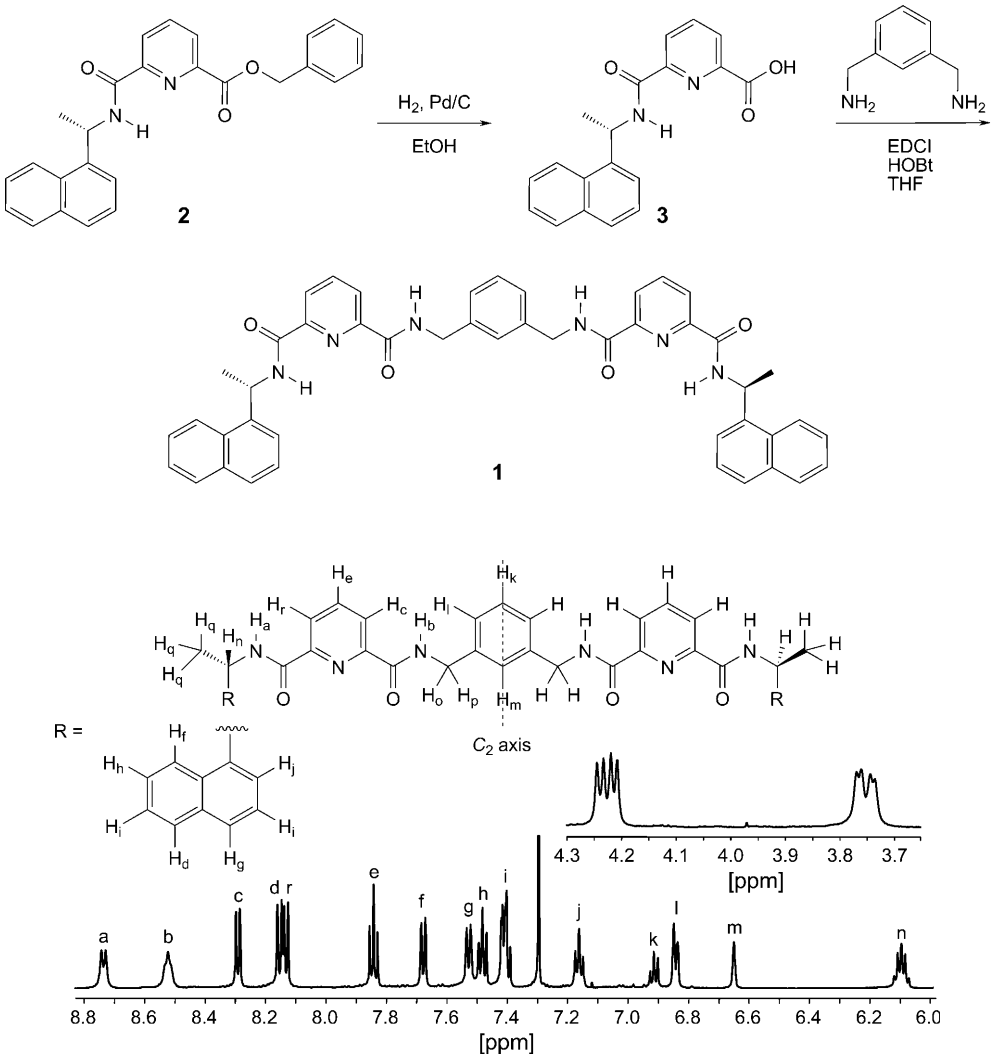

Fig. 1. *Partial* ^{1}*H-NMR spectrum* (600 MHz, $CDCl_3$) *of* **1**

21055 M^{-1} cm^{-1}), with a small shoulder at 293 nm. Excitation at the 281 nm transition gave rise to a fluorescence-emission spectrum consisting of two main bands at 333 and 427 nm. We next monitored the changes in the ground and the excited states upon titrating **1** ($1.0 \cdot 10^{-5}$ M) with Sm^{III}, Eu^{III}, and Tb^{III} (as their corresponding $Ln(SO_3CF_3)_3$ stock solutions). The overall changes observed in the absorption spectra of **1** for the titration with Eu^{III} are shown in *Fig. 2*, which demonstrates significant changes upon binding of Eu^{III} to **1**. The long-wavelength absorption band was particularly affected (see inset in *Fig. 2*), where the absorption was bathochromically shifted and a new

shoulder was formed at longer wavelength, with a pseudo-isosbestic point at 296 nm. A clearer isosbestic point was also observed at 265 nm. These changes were analyzed by fitting the global changes in *Fig. 2* by means of the nonlinear regression analysis program SPECFIT (*Fig. 3,a*). The speciation-distribution diagram resulting from these fits showed the presence of three major species in solution (*Fig. 3,b*). Of these, within the addition of $0.2 \rightarrow 0.8$ equiv. of Eu^{III}, the most predominant one was a ligand/metal 3 : 2 species, being formed in over 80% at 0.67 equiv. of Eu^{III}. The stoichiometry of this species corresponds to the formation of a dimetallic triple-stranded helicate, where

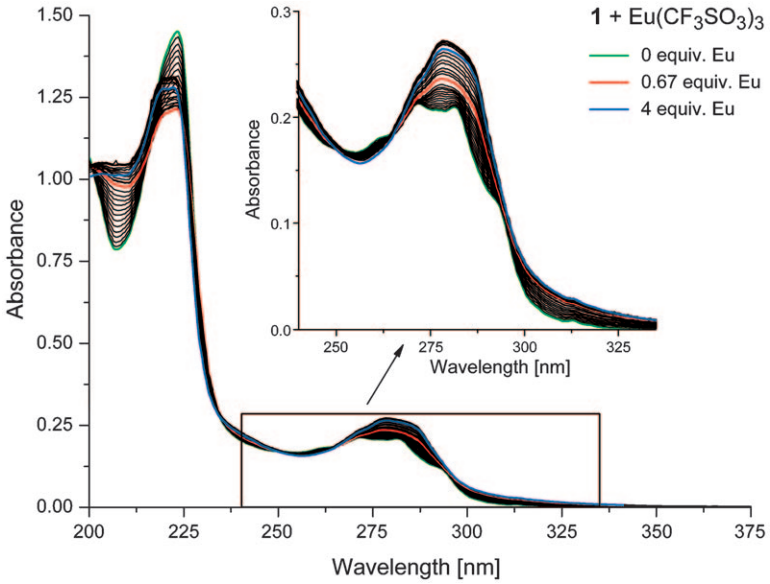

Fig. 2. *Changes in the absorption spectra of* **1** ($1.0 \cdot 10^{-5}$ M) *upon titrating with* $Eu(SO_3CF_3)_3$ ($0 \rightarrow 4$ equiv.) *in MeCN at room temperature.* Inset: Changes in the long-wavelength absorption band.

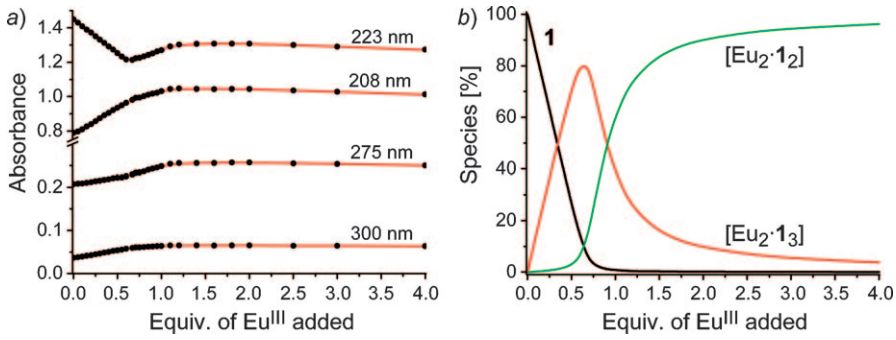

Fig. 3. a) *Experimental binding isotherms for the UV/VIS titration of* **1** ($1.0 \cdot 10^{-5}$ M) *with* $Eu(SO_3CF_3)_3$ ($0 \rightarrow 4$ equiv.) *in MeCN at room temperature and their corresponding fit by means of SPECFIT* (—). b) *Speciation-distribution diagram obtained from the fit.*

each of the Eu^{III} ion would be located within a nine-coordinated environment, bound to the two carboxamide groups and the central pyridine N-atom of each ligand giving $[Eu_2 \cdot \mathbf{1}_3]$. However, at higher concentration, the formation of the ligand/metal 2:2 species $[Eu_2 \cdot \mathbf{1}_2]$ became dominant in solution, being formed in over 90% after the addition of 3 equiv. of Eu^{III}. Similarly, the titrations of **1** with Sm^{III} and Tb^{III} both gave rise to identical changes in the absorption spectra as seen for Eu^{III} in *Fig. 2*, from which speciation-distribution diagrams showed again the presence of two main metallic species, corresponding to the formation of $[Ln_2 \cdot \mathbf{1}_3]$ and $[Ln_2 \cdot \mathbf{1}_2]$, respectively.

From the above results, we determined the stability constants (expressed as $\log \beta_{M/L}$) for the formation of all of the $[Ln_2 \cdot \mathbf{1}_3]$ and $[Ln_2 \cdot \mathbf{1}_2]$ complexes. In the case of Eu^{III}, the $[Eu_2 \cdot \mathbf{1}_3]$ helicate was formed with a high binding constant $\log \beta_{2:3} = 27.3$ (± 0.3), while the $[Eu_2 \cdot \mathbf{1}_2]$ complex was formed with a $\log \beta_{2:2} = 20.5$ (± 0.2). These are of a magnitude comparable to those reported by *Bünzli* and co-workers for triple-stranded helicates, based on the use of bis-benzimidazole ligands [16]. In a similar manner, binding constants for the titrations of Sm^{III} and Tb^{III} were determined and found to be of similar magnitude to that seen for Eu^{III} (*Table*).

Table. *Binding Constants Obtained by Fitting Various Spectroscopic Data*

		Absorption		Luminescence[a])	
	Species	$\log \beta_{M/L}$	% Species for M/L 2:3	$\log \beta_{M/L}$	% Species for M/L 2:3
Sm^{III}	$\log \beta_{2:2}$	20.2 ± 0.2	23	21.8 ± 0.2	19
	$\log \beta_{2:3}$	26.4 ± 0.3	65	28.3 ± 0.3	72
Eu^{III}	$\log \beta_{2:2}$	20.5 ± 0.2	13	21.7 ± 0.2	10
	$\log \beta_{2:3}$	27.3 ± 0.3	80	28.7 ± 0.3	84
Tb^{III}	$\log \beta_{2:2}$	20.3 ± 0.2	17	[b])	[b])
	$\log \beta_{2:3}$	26.8 ± 0.3	73	[b])	[b])
Lu^{III}	$\log \beta_{2:2}$	19.0 ± 0.3	10	19.8 ± 0.3	4
	$\log \beta_{2:3}$	25.8 ± 0.4	81	27.4 ± 0.4	92
	$\log \beta_{2:1}$	–	–	12.7 ± 0.2	< 1

[a]) Obtained by fitting the changes in the metal-centred emission, except for Lu^{III} where the fluorescence emission was used. [b]) The evolution of the Tb^{III} luminescence could not be fitted satisfyingly.

Having investigated the changes in the absorption spectra of **1**, we next investigated the changes in the fluorescence-emission spectra of **1** upon titration with Sm^{III}, Eu^{III}, and Tb^{III}. The overall changes observed for the titration with Eu^{III} are shown in *Fig. 4*, and clearly establish significant changes in the fluorescence upon formation of the Eu^{III} helicates. The long-wavelength emission was particularly affected, being almost 80% quenched after the addition of *ca.* 0.7 equiv. of Eu^{III}, which corresponds to the expected metal/ligand 2:3 stoichiometry and, hence, to the formation of the $[Eu_2 \cdot \mathbf{1}_3]$ helicate. However, unlike that seen in the absorption spectra above, we were unable to obtain reliable binding constants for the formation of both the $[Eu_2 \cdot \mathbf{1}_3]$ and $[Eu_2 \cdot \mathbf{1}_2]$ complexes upon fitting these fluorescence changes with SPECFIT. In a similar manner, the fitting of the changes observed in the fluorescence emission of **1** upon titration with Sm^{III} and Tb^{III} only resulted in binding constants carrying an unacceptable error.

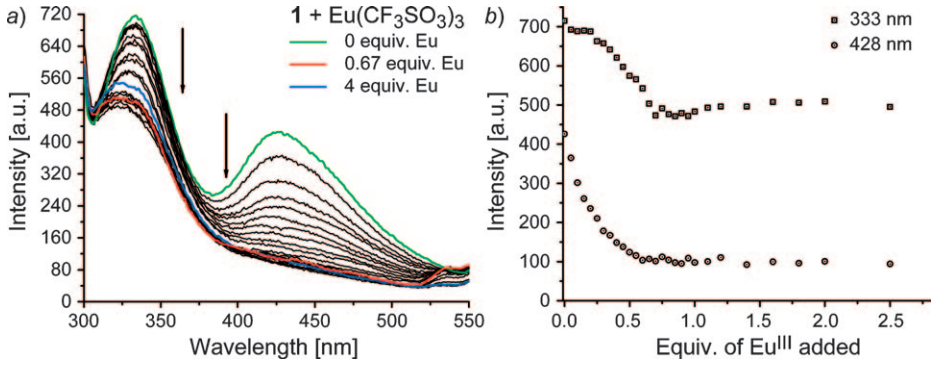

Fig. 4. a) *Changes in the fluorescence emission of* **1** ($1.0 \cdot 10^{-5}$ M) *upon titrating with* $Eu(SO_3CF_3)_3$ ($0 \rightarrow 4$ equiv.) *in MeCN at room temperature.* b) *Experimental binding isotherms of the fluorescence-emission intensity at* λ *333 and 428 nm* vs. *the equiv. of* $Eu(SO_3CF_3)_3$.

Because of this, we also carried out a titration of **1** with Lu^{III}, which should result in the formation of helicates displaying no metal-centred emission. Hence, the formation of either the $[Lu_2 \cdot \mathbf{1}_3]$ or $[Lu_2 \cdot \mathbf{1}_2]$ complex would not be expected to perturb the singlet excited state of **1** in the manner to that observed above for Sm^{III}, Eu^{III}, or Tb^{III}. The results from this titrations are shown in *Fig. 5*, and demonstrate that the fluorescence of **1** was dramatically affected (*Fig. 5,a*), and unlike that seen above, where the λ_{max} at 425 nm was quenched, the concomitant formation of a new red-shifted band with λ_{max} at *ca.* 513 nm, was observed. Furthermore, from the changes in the emission spectra at various wavelengths (*Fig. 5,b*), we were able to verify the successful formation of $[Lu_2 \cdot \mathbf{1}_3]$ in solution. Moreover, fitting the changes observed in *Fig. 5,a*, with SPECFIT gave $\log \beta_{2:3} = 27.4$ (± 0.4) and $\log \beta_{2:2} = 19.8$ (± 0.3) for $[Lu_2 \cdot \mathbf{1}_3]$ and $[Lu_2 \cdot \mathbf{1}_2]$, respectively, which are in good agreement with that observed from the ground-state titration of Eu^{III} above. In contrast, the changes in the absorption spectra were identical to those seen for Eu^{III} in *Fig. 2*, and analysis of the changes with SPECFIT indeed gave similar binding constants to those obtained from the absorption spectra of **1** upon titration with

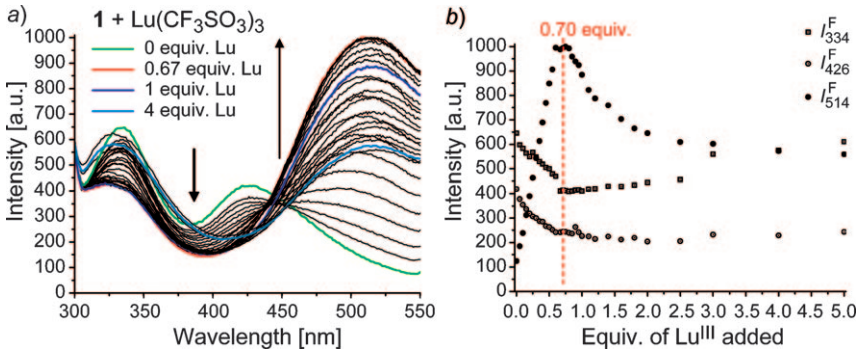

Fig. 5. a) *Changes in the fluorescence emission of* **1** ($1.0 \cdot 10^{-5}$ M) *upon titrating with* $Lu(SO_3CF_3)_3$ ($0 \rightarrow 4$ equiv.) *in MeCN at room temperature.* b) *Experimental binding isotherms of the fluorescence-emission intensity at* λ *334, 428, and 514 nm* vs. *the equiv. of* $Lu(SO_3CF_3)_3$

Sm^{III}, Eu^{III}, and Tb^{III}. These results clearly demonstrate that even in the absence of an energy acceptor such as Sm^{III}, Eu^{III}, and Tb^{III}, the fluorescence emission is dramatically affected, giving rise to the formation of the long-wavelength emission, which we assign to the formation of the helical structure in solution. Hence we next evaluated the evolution of the lanthanide emission in solution upon formation of $[Ln_2 \cdot \mathbf{1}_3]$ and $[Ln_2 \cdot \mathbf{1}_2]$ complexes.

3. *Observing the Formation of $[Ln_2 \cdot \mathbf{1}_3]$ and $[Ln_2 \cdot \mathbf{1}_2]$ by Monitoring the Lanthanide-Centred Emission.* In a similar manner to that described above, the evolution in the delayed lanthanide luminescence arising from the Sm^{III}, Eu^{III}, and Tb^{III} ions was monitored upon formation of these helical species with **1**, upon exciting the naphthalene antennae at 281 nm. The changes observed for Eu^{III} are shown in *Fig. 6,a*, monitoring the characteristic emission bands appearing at 580, 595, 616, 650, and

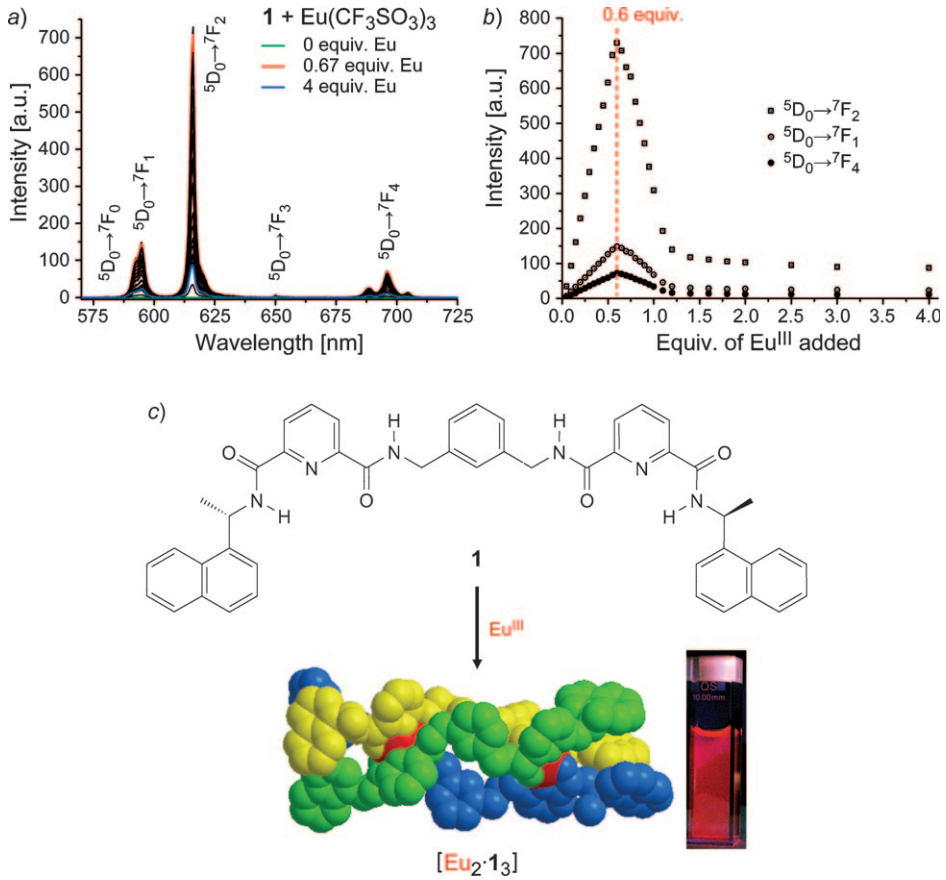

Fig. 6. a) *Changes in the Eu^{III} phosphorescence spectra upon titrating* **1** ($1.0 \cdot 10^{-5}$ M) *with $Eu(SO_3CF_3)_3$* ($0 \rightarrow 4$ equiv.) *in MeCN at room temperature.* b) *Experimental binding isotherms of the Eu^{III} phosphorescence-emission intensity at λ 595* ($^5D_0 \rightarrow {}^7F_1$), *616* ($^5D_0 \rightarrow {}^7F_2$), *and 696 nm* ($^5D_0 \rightarrow {}^7F_4$) vs. *the equiv. of $Eu(SO_3CF_3)_3$.* c) *Formation of $[Eu_2 \cdot \mathbf{1}_3]$ and red emission of its solution under a UV/VIS lamp.*

696 nm, respectively, and assigned to the deactivation of the $^5D_0$ excited state to the ^7F_J ground states ($J = 0$, 1, 2, 3 and 4). Of these, the $^5D_0 \rightarrow {}^7F_1$, $^7F_2$, and $^7F_4$ were the most intense. Analysis of their emission intensity as a function of the equiv. of Eu^{III} added (*Fig. 6,b*) showed that the Eu^{III} emission evolves rapidly up to the addition of 0.6–0.7 equiv., after which the emission decreases until it reaches a plateau at *ca.* 1.2 equiv. of Eu^{III}. This suggests the initial formation of the desired $[Eu_2 \cdot \mathbf{1}_3]$ helicate, after which the $[Eu_2 \cdot \mathbf{1}_2]$ becomes the dominant species in solution. The helicate $[Eu_2 \cdot \mathbf{1}_3]$ was also synthesized *in situ* by mixing the correct stoichiometry of **1** with Eu^{III} ($[[Eu_2 \cdot \mathbf{1}_3]] = 1.33 \cdot 10^{-5}$ M), and the changes in the Eu^{III} emission were monitored over 5 h. The results from this experiment demonstrated the immediate formation of the helicate in solution (within seconds) and that the Eu^{III} emission was unchanged over this time period, clearly indicating the kinetic stability of the $[Eu_2 \cdot \mathbf{1}_3]$ species in solution. Moreover, this solution displayed the characteristic red emission under a UV/VIS lamp, as demonstrated in *Fig. 6,c*. We also measured the decay of the $^5D_0$ excited state upon excitation at 281 nm, at different ligand-to-metal ratios and fitting the data with both mono- and bi-exponential functions. The results demonstrate that, up to 0.6 equiv. of Eu^{III}, the decay was best fitted to mono-exponential decay, with a lifetime of 1.57 ms measured for the $[Eu_2 \cdot \mathbf{1}_3]$ helicate. At higher concentrations of Eu^{III}, the decay was, however, best fitted to the bi-exponential function, which is in accordance to our observation that a second minor species, $[Eu_2 \cdot \mathbf{1}_2]$, is formed in solution (which becomes a dominant contributor at higher concentrations).

The overall results from the titrations of **1** with Sm^{III} and Tb^{III} are shown in *Fig. 7,a* and *b*, respectively, and also demonstrate the effective sensitization of their $^4G_{5/2}$ and $^5D_4$ excited states, respectively, and the evolution of a line-like emission bands at long wavelengths upon excitation of the antennae. Analysis of the changes in the Sm^{III} transitions ($^4G_{5/2} \rightarrow {}^6H_{5/2}$, $^6H_{7/2}$, $^6H_{9/2}$, and $^6H_{11/2}$) are shown in *Fig. 8,a*, and demonstrate the initial formation of triple-stranded helicate $[Sm_2 \cdot \mathbf{1}_3]$ followed by the formation of the $[Sm_2 \cdot \mathbf{1}_2]$ complex at higher concentration. In contrast to these results, the changes in the Tb^{III} emission were strikingly different (*Fig. 8,b*) which demonstrates that only very minor changes were observed up to the addition of 0.6 equiv. of Tb^{III}, after which

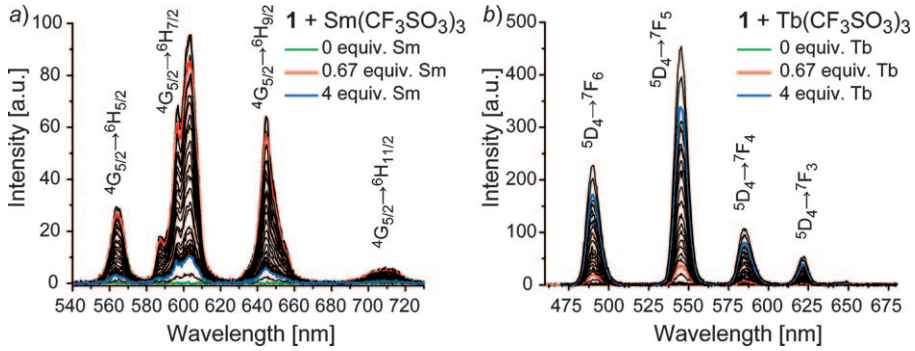

Fig. 7. a) *Changes in the Sm^{III} phosphorescence spectra upon titrating* **1** ($1.0 \cdot 10^{-5}$ M) *with $Sm(SO_3CF_3)_3$* (0 → 4 equiv.) *in MeCN at room temperature.* b) *Changes in the Tb^{III} phosphorescence spectra upon titrating* **1** ($1.0 \cdot 10^{-5}$ M) *with $Tb(SO_3CF_3)_3$* (0 → 12 equiv.) *in MeCN at room temperature.*

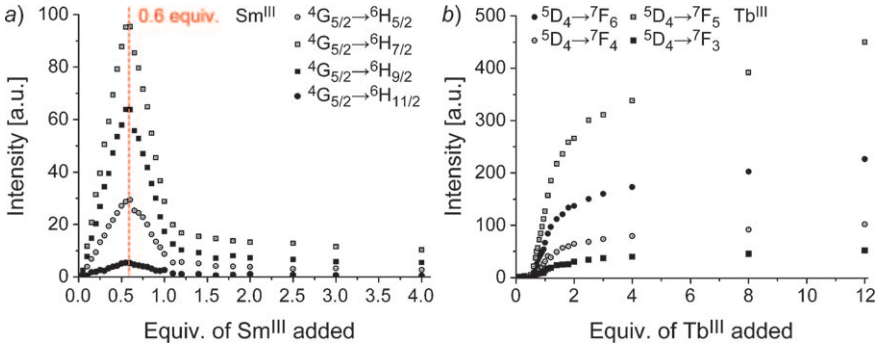

Fig. 8. a) *Experimental binding isotherms of the Sm^{III} phosphorescence-emission intensity at λ 564* ($^4G_{5/2} \rightarrow {}^6H_{5/2}$), *604* ($^4G_{5/2} \rightarrow {}^6H_{7/2}$), *645* ($^4G_{5/2} \rightarrow {}^6H_{9/2}$), *and 710 nm* ($^4G_{5/2} \rightarrow {}^6H_{11/2}$) vs. *the equiv. of Sm(SO$_3$CF$_3$)$_3$.* b) *Experimental binding isotherms of the Tb^{III} phosphorescence-emission intensity at λ 490* ($^5D_4 \rightarrow {}^7F_6$), *545* ($^5D_4 \rightarrow {}^7F_5$), *585* ($^5D_4 \rightarrow {}^7F_4$), *and 622 nm* ($^5D_4 \rightarrow {}^7F_3$) vs. *the equiv. of Tb(SO$_3$CF$_3$)$_3$.*

the Tb^{III} emission intensity rapidly increased between 0.6 → 2.5 – 3 equiv. of Tb^{III}. When these measurements were repeated with samples that were equilibrated over 24 h, the same behaviour was observed. Hence, this difference is not due to slow kinetics. Furthermore, the formation of the desired dimetallic Tb^{III} helicate was ascertained by monitoring the changes observed in the UV/VIS absorption spectra; consequently, we attribute these changes to a most likely occurring energy back transfer from the metal to the ligand. We are in the process of investigating this phenomenon further.

The changes in the Eu^{III} and the Sm^{III} emissions shown above were fitted with SPECFIT. The results for Eu^{III} (*Fig. 9,a*) demonstrate that an excellent fit was observed, from which the binding constants for the formation of the [Eu$_2 \cdot$ **1**$_3$] helicate and [Eu$_2 \cdot$ **1**$_2$] were determined as $\log \beta_{2:3} = 28.7$ (± 0.3) and $\log \beta_{2:2} = 21.7$ (± 0.2), respectively, which are in good agreement with that determined from the changes in the absorption spectra. These values are summarized in the *Table*. From these, the speciation-distribution diagram was deduced (*Fig. 9,b*), which again matched that

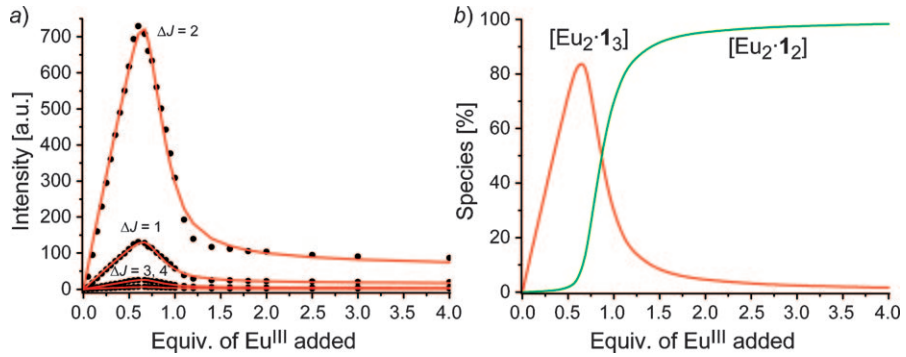

Fig. 9. a) *Experimental binding isotherms for the changes in the Eu^{III} phosphorescence-emission spectra upon titrating* **1** ($1.0 \cdot 10^{-5}$ M) *with Eu(SO$_3$CF$_3$)$_3$* (0 → 4 equiv.) *in MeCN at room temperature and their corresponding fit by means of SPECFIT* (—). b) *Speciation-distribution diagram obtained from the fit.*

derived from the absorption changes (*Fig. 3,b*). In a similar manner, the fitting of the changes observed for Sm^{III} also resulted in an excellent fit, from which binding constants $\log \beta_{2:3} = 28.3$ (± 0.3) and $\log \beta_{2:2} = 21.8$ (± 0.2) for the formation of the $[Sm_2 \cdot \mathbf{1}_3]$ helicate and $[Sm_2 \cdot \mathbf{1}_2]$, respectively, were determined. These are in excellent agreement with that found for Eu^{III}. From these values, the speciation-distribution diagram was constructed, which showed a comparable trend to that shown in *Fig. 9,b*. Overall, these results clearly demonstrate that these helicates are formed in high yield and with high binding constants.

Conclusions. – The synthesis of a C_2-symmetrical ligand **1** was undertaken and achieved in few and high-yielding steps. We showed that upon titrating **1** with various lanthanide ions, significant changes were observed in the absorption and the fluorescence-emission spectra of **1**. Analysis of the changes in the absorption spectrum revealed that significant changes occurred upon the addition of $0 \rightarrow 0.7$ equiv. of Ln^{III} ions, suggesting the formation of a metal/ligand 2:3 stoichiometry between Ln^{III} and **1**. Further changes were observed up to 1 equiv. of Ln^{III}. Analysis of these global changes with the nonlinear regression analysis program SPECFIT confirmed the formation of dinuclear triple-stranded helicates for all Ln^{III} (Ln = Sm, Eu, Tb, and Lu) with average binding constants $\log \beta \approx 27$, and the formation of a 2:2 species at higher concentrations of these ions with $\log \beta \approx 20$ (see details in the *Table*). The changes in the fluorescence emission also confirmed the formation of two species in solution; however, we were unable to fit the changes induced by Sm^{III}, Eu^{III}, and Tb^{III}, all of which can give rise to metal-centred luminescence. However, we were able to analyse the fluorescence changes seen for Lu^{III}. While these changes were somewhat different to that observed for the above ions, the analysis resulted in a good fit to these changes, which confirmed the formation of $[Lu_2 \cdot \mathbf{1}_3]$ and $[Lu_2 \cdot \mathbf{1}_2]$ in solution. In a similar manner, the delayed lanthanide emission was also monitored. Only minor changes were seen in the Tb^{III} emission up to the addition of 0.7 equiv. of Tb^{III}, after which the emission gradually increased up to the addition of 2.5–3 equiv. Consequently, we were unable to determine from these data the binding constants and then the speciation distribution in solution for the formation of $[Tb_2 \cdot \mathbf{1}_3]$ and $[Tb_2 \cdot \mathbf{1}_2]$. However, in the case of Sm^{III} and Eu^{III}, their respective lanthanide emission was 'switched on' upon formation of $[Sm_2 \cdot \mathbf{1}_3]$ and $[Eu_2 \cdot \mathbf{1}_3]$, as well as $[Sm_2 \cdot \mathbf{1}_2]$ and $[Eu_2 \cdot \mathbf{1}_2]$, respectively, with binding constants that were determined to be of similar magnitude to that determined from the changes observed in the UV/VIS absorption spectra. In summary, we have developed novel lanthanide luminescent dimetallic triple-stranded helicates from a simple ligand **1**, and demonstrated that these helicates are formed in solution in high yield, while possessing high binding constants. We are currently in the process of developing other related systems and conjugates for the formation of novel supramolecular architectures.

We thank the *SFI* (*Science Foundation Ireland*), *HEA* (*Higher Education Authority*; for PRTLI Cycle 3 CSCB funding to *T. G.* and a scholarship to *F. S.*), *IRCSET* (*The Irish Research Council for Science, Engineering & Technology*; for a postdoctoral fellowship to *S. C.*), Queen's University of Belfast and Trinity College Dublin for financial support, and Dr. *John E. O'Brian* (Trinity College Dublin) for performing NMR measurements.

Experimental Part

General. All chemicals were purchased from commercial sources and unless specified used without further purification. Stock solns. of lanthanides at a concentration around $5 \cdot 10^{-3}$ M were prepared just before use in HPLC-grade MeCN from the corresponding $Ln(CF_3SO_3)_3$ salts (Ln = Sm, Eu, Tb, and Lu). The lanthanide triflate salts were dried under vacuum over P_2O_5 prior to use. IR Spectra: *Perkin-Elmer-Spectrum-One* FT-IR spectrometer equipped with a *Universal-ATR* sampling accessory; solid samples were recorded directly as neat samples; in cm^{-1}. NMR Spectra: *Bruker-DPX-400-Avance* spectrometer (400.13 (^{1}H) and 100.6 MHz (^{13}C)), or *Bruker-AV-600* spectrometer (600.13 (^{1}H) and 150.2 MHz (^{13}C)); in commercially available deuterated solvents; δ in ppm rel. to $SiMe_4$ (= 0 ppm) referenced rel. to the internal solvent signals, J in Hz; data were processed with *Bruker* Win-NMR 5.0 and Topspin 2.1 softwares. ESI-MS: *Micromass-LCT* spectrometer, running MassLynx NT V 3.4 on a *Waters-600* controller connected to a 996 photodiode array detector with HPLC-grade MeCN as carrier solvents; all experiments in positive-ion mode; accurate molecular masses by a peak-matching method, with leucine enkephaline (H-Tyr-Gly-Gly-Phe-Leu-OH) as the standard internal reference (m/z 556.2771), and reported within 5 ppm. Elemental analyses were carried out at the Microanalytical Laboratory, School of Chemistry and Chemical Biology, University College Dublin.

UV/VIS-Absorption and Emission Data. Absorption spectra were measured in 1-cm quartz cuvettes with a *Varian-Cary-50* spectrophotometer. Baseline correction was applied for all spectra. Emission spectra and lifetimes were measured with a *Varian-Cary-Eclipse* luminescence spectrometer. In both experiments, the temp. was kept constant at 298 K throughout the measurements by using a thermostated unit block. In a typical spectrophotometric titration, 2.7 ml of ligand **1** at a concentration of $1.0 \cdot 10^{-5}$ M was titrated with a *ca.* $5 \cdot 10^{-4}$ M Ln^{III} soln. (Ln = Sm, Eu, Tb, or Lu). Treatment of the resulting data with the nonlinear least-squares regression-analysis program SPECFIT® then allowed the determination of the conditional stability constants for the formation of the different metal complexes.

6-{{[(1S)-1-(Naphthalen-1-yl)ethyl]amino}carbonyl}pyridine-2-carboxylic Acid Benzyl Ester (**2**). To a stirred soln. of (1*S*)-1-(naphthalen-1-yl)ethylamine (0.630 ml, 3.9 mmol) in anh. THF (30 ml), HOBt (= 1-hydroxy-1*H*-benzotriazole; 0.527 g, 3.9 mmol) and pyridine-2,6-dicarboxylic acid 2-benzyl ester (1 g, 3.9 mmol) were added. This soln. was then stirred for further 30 min at 0° under Ar. To this soln., EDCI · HCl (= 1-ethyl-3-[3-(dimethylamino)propyl]carbodiimide hydrochloride; 0.785 g, 4.1 mmol) and Et_3N (0.571 ml, 4.1 mmol) were added, and the mixture was stirred at 0° for 30 min and then at r.t. for 18 h. The insoluble residue was filtered off and the filtrate concentrated. CH_2Cl_2 was added to the crude oil, the soln. washed twice with 1M HCl, sat. $NaHCO_3$ soln., and H_2O, dried, and concentrated, and the crude product, if necessary, purified by flash column chromatography (neutral silica gel): **2** (1.26 g, 79%). Pale yellow oil. IR (NaCl): 3381, 1718, 1651, 1588, 1305, 1155, 1077, 966, 722. ^{1}H-NMR (400 MHz, $CDCl_3$, 298.2 K): 8.51 (*d*, *J* = 8.5, NH); 8.44 (*d*, *J* = 7.5, 1 pyr-H); 8.23 (*d*, *J* = 7.5, 1 nap-H, 1 pyr-H); 8.00 (*t*, *J* = 7.5, 1 pyr-H); 7.89 (*d*, *J* = 8.5, 1 nap-H); 7.83 (*d*, *J* = 8.5, 1 nap-H); 7.64 (*d*, *J* = 7.0, 1 nap-H); 7.57 – 7.38 (*m*, 3 nap-H, Ph); 6.22 – 6.15 (*m*, MeC*H*); 5.42 (*s*, CH_2); 1.82 (*d*, *J* = 7.0, Me). ^{13}C-NMR (100 MHz, $CDCl_3$, 298.2 K): 163.7; 161.9; 149.7; 146.0; 138.0; 137.9; 134.9; 133.5; 130.6; 128.4; 128.2; 128.0; 127.8; 127.7; 126.8; 126.0; 125.3; 125.1; 124.9; 122.9; 122.2; 67.0; 44.5; 20.9. HR-ESI-MS: 433.1549 ($[M + Na]^+$, $C_{26}H_{22}N_2NaO_3^+$; calc. 433.1528).

6-{{[(1S)-1-(Naphthalen-1-yl)ethyl]amino}carbonyl}pyridine-2-carboxylic Acid (**3**). The free acid **3**, was obtained by hydrogenation of **2** (1.22 g) in MeOH in the presence of 10% Pd/C (0.1 equiv.) under 3 atm of H_2. The resulting mixture was passed through a *Celite* filter and the filtrate concentrated: **3** (0.85 g, 90%). Yellow solid. M.p. 116 – 120°. IR (neat): 3282, 3049, 2977, 2936, 1751, 1651, 1524, 1452, 1345, 1255, 1172, 1118, 1076, 1000, 921, 846, 799, 776, 745, 681. ^{1}H-NMR (400 MHz, $CDCl_3$, 298.2 K): 8.49 (*d*, *J* = 8.5, 1 NH); 8.44 (*d*, *J* = 7.5, 1 pyr-H); 8.23 (*d*, *J* = 8.5, 1 nap-H); 8.19 (*d*, *J* = 7.5, 1 pyr-H); 7.99 (*t*, *J* = 7.5, 1 pyr-H); 7.88 (*d*, *J* = 8.0, 1 nap-H); 7.82 (*d*, *J* = 8.0, 1 nap-H); 7.65 (*d*, *J* = 7.0, 1 nap-H); 7.56 (*t*, *J* = 7.0, 1 nap-H); 7.50 – 7.45 (*m*, 2 nap-H); 6.21 – 6.15 (*m*, MeC*H*); 1.83 (*d*, *J* = 7.0, Me). ^{13}C-NMR (100 MHz, $CDCl_3$, 298.2 K): 163.3; 161.5; 148.8; 144.5; 139.1; 137.2; 133.4; 130.6; 128.4; 128.1; 126.4; 126.2; 126.2; 125.4; 124.8; 122.7; 122.4; 44.6; 20.3. HR-ESI-MS: 343.1061 ($[M + Na]^+$, $C_{19}H_{16}N_2NaO_3^+$; calc. 343.1059). Anal. calc. for $C_{19}H_{16}N_2O_3 \cdot 0.5\ H_2O$: C 69.29, H 5.20, N 8.51; found: C 69.23, H 5.13, N 8.34.

N^2,$N^{2'}$-*[1,3-Phenylenebis(methylene)]bis[*N^6-*[(1*S*)-1-(naphthalen-1-yl)ethyl]pyridine-2,6-dicarboxamide* (**1**). To a mixture of 1,3-xylenediamine (= benzene-1,3-methanamine; 62 µl, 0.47 mmol) and **3** (0.3 g, 0.94 mmol), HOBt (0.1324 g, 0.98 mmol) in THF (*ca.* 25 ml), EDCI · HCl (0.187 g, 0.98 mmol), Et_3N (0.136 ml, 0.98 mmol), and DMAP (*N*,*N*-dimethylpyridin-4-amine; 68.4 mg, 0.56 mmol) were added after cooling the mixture at 0°. The mixture was stirred for 24 h and then filtered through a *Celite* pad. The filtrate was concentrated, the crude oil dissolved in CH_2Cl_2, the soln. washed three times with aq. 1M HCl, sat. $NaHCO_3$ soln., and H_2O, dried ($MgSO_4$), and concentrated, and the residue dried under vacuum to give a yellow oil (186 mg, 54% yield). This oil was dissolved in few ml of CH_2Cl_2/$CHCl_3$ and added dropwise to swirling 100 ml of dry Et_2O. The off-white precipitate that was formed was collected by filtration through a *Hirsch* funnel: **1** (87 mg, 0.119 mmol, 25%). Yellow solid. IR (neat): 3300, 3053, 2976, 2933, 2084, 1658, 1598, 1521, 1444, 1411, 1398, 1373, 1339, 1309, 1238, 1174, 1118, 1076, 1000, 920, 844, 800, 777, 750, 676. ^{1}H-NMR (600.1 MHz, $CDCl_3$, 298 K): 8.70 (*d*, *J* = 8.8, 2 NH); 8.53–8.44 (*m*, 2 NH); 8.26 (*d*, *J* = 7.3, 2 pyr-H); 8.12 (*d*, *J* = 8.8, 2 nap-H); 8.10 (*d*, *J* = 7.3, 2 pyr-H); 7.81 (*t*, *J* = 7.7, 2 pyr-H); 7.64 (*d*, *J* = 8.0, 2 nap-H); 7.49 (*d*, *J* = 8.1, 2 nap-H); 7.45 (*t*, *J* = 7.7, 2 nap-H); 7.41–7.34 (*m*, 4 nap-H); 7.13 (*t*, *J* = 7.7, 2 nap-H); 6.88 (*t*, *J* = 7.7, 1 Ar-H); 6.08–6.04 (*m*, MeC*H*); 4.18–4.22 (*m*, CH_2); 3.72 (*m*, CH_2); 1.57 (*d*, *J* = 6.6, 2 Me). ^{13}C-NMR (150.9 MHz, $CDCl_3$, 298 K): 164.3; 163.0; 149.2; 148.7; 139.0; 138.6; 138.4; 134.2; 131.6; 129.1; 128.5; 126.9; 126.6; 126.1; 125.7; 125.3; 125.2; 123.8; 123.4; 45.3; 43.2; 20.7. HR-ESI-MS: 763.2815 ($[M + Na]^+$, $C_{46}H_{40}N_6NaO_4^+$; calc. 763.3009). Anal. calc. for $C_{46}H_{40}N_6O_4 \cdot 0.27\ CHCl_3$: C 71.89, H 5.25, N 10.87; found: C 71.89, H 5.35, N 10.84.

REFERENCES

[1] C. M. G. dos Santos, A. J. Harte, S. J. Quinn, T. Gunnlaugsson, *Coord. Chem. Rev.* **2008**, *252*, 2512; J. P. Leonard, C. B. Nolan, F. Stomeo, T. Gunnlaugsson, *Top. Curr. Chem.* **2007**, *281*, 1; T. Gunnlaugsson, F. Stomeo, *Org. Biomol. Chem.* **2007**, *5*, 1999; T. Gunnlaugsson, J. P. Leonard, *Chem. Commun.* **2005**, 3114; J. P. Leonard, T. Gunnlaugsson, *J. Fluoresc.* **2005**, *15*, 585.

[2] J.-C. G. Bünzli, *Chem. Lett.* **2009**, *38*, 104; J.-C. G. Bünzli, *Acc. Chem. Res.* **2006**, *39*, 53; S. Comby, J.-C. G. Bünzli, in 'Handbook of the Chemistry and Physics of Rare Earths', Eds. K. A. Gschneider, J.-C. G. Bünzli, and V. K. Pecharsky, Elsevier, Amsterdam, 2007, Vol. 37.

[3] S. Faulkner, L. S. Natrajan, W. S. Perry, D. Sykes, *Dalton Trans.* **2009**, 3890; M. D. Ward, *Coord. Chem. Rev.* **2007**, *251*, 1663.

[4] S. Goetz, P. E. Kruger, *Dalton Trans.* **2006**, 1277.

[5] A. I. Prikhod'ko, F. Durola, J.-P. Sauvage, *J. Am. Chem. Soc.* **2008**, *130*, 448.

[6] K. S. Chichak, S. J. Cantrill, A. R. Pease, S.-H. Chui, G. W. V. Cave, J. L. Atwood, J. F. Stoddart, *Science (Washington, DC, U.S.)* **2004**, *304*, 1308.

[7] E. R. Kay, D. A. Leigh, F. Zerbetto, *Angew. Chem., Int. Ed.* **2007**, *46*, 72.

[8] M. Albrecht, R. Fröhlich, *Bull. Chem. Soc. Jpn.* **2007**, *80*, 797; J. R. Nitschke, *Acc. Chem. Res.* **2007**, *40*, 103; M. Fujita, M. Tominaga, A. Hori, B. Therrien, *Acc. Chem. Res.* **2005**, *38*, 369.

[9] K. A. O'Donoghue, J. M. Kelly, P. E. Kruger, *Dalton Trans.* **2004**, 13.

[10] R. J. Hill, D.-L. Long, N. R. Champness, P. Hubberstey, M. Schröder, *Acc. Chem. Res.* **2005**, *38*, 335.

[11] T. K. Ronson, H. Adams, L. P. Harding, S. J. A. Pope, D. Sykes, S. Faulkner, M. D. Ward, *Dalton Trans.* **2007**, 1006; O. Mamula, M. Lama, S. G. Telfer, A. Nakamura, R. Kuroda, S. Stoeckli-Evans, R. Scopelitti, *Angew. Chem., Int. Ed.* **2005**, *44*, 2527; J. J. Lessmann, W. D. Horrocks Jr., *Inorg. Chem.* **2000**, *39*, 3114.

[12] T. Lazarides, D. Sykes, S. Faulkner, A. Barbieri, M. D. Ward, *Chem.–Eur. J.* **2008**, *14*, 9389; S. G. Baca, H. Adams, D. Sykes, S. Faulkner, M. D. Ward, *Dalton Trans.* **2007**, 2419; M. Mehlstäubl, G. S. Kottas, S. Collella, L. De Cola, *Dalton Trans.* **2008**, 2385; S. J. A. Pope, B. J. Coe, S. Faulkner, *Chem. Commun.* **2004**, 1550; P. Coppo, M. Duati, V. N. Kozhevnikov, J. W. Hofstraat, L. De Cola, *Angew. Chem., Int. Ed.* **2005**, *44*, 1806; S. J. A. Pope, B. J. Coe, S. Faulkner, R. H. Laye, *Dalton Trans.* **2005**, 1482; N. M. Shavaleev, S. J. A. Pope, Z. R. Bell, S. Faulkner, M. D. Ward, *Dalton Trans.* **2003**, 808; Y. Bretonnière, M. Mazzanti, R. Wietzke, J. Pécaut, *Chem. Commun.* **2000**, 1543.

[13] M. Albrecht, O. Osetska, R. Fröhlich, J.-C. G. Bünzli, A. Aebischer, F. Gumy, J. Hamacek, *J. Am. Chem. Soc*. **2007**, *129*, 14178; P. B. Glover, P. R. Ashton, L. J. Childs, A. Rodger, M. Kercher, R. M. Williams, L. De Cola, Z. Pikramenou, *J. Am. Chem. Soc.* **2003**, *125*, 9918.

[14] a) E. Deiters, B. Song, A. S. Chauvin, C. D. B. Vandevyver, F. Gumy, J.-C. G. Bünzli, *Chem.–Eur. J.* **2009**, *15*, 885; b) J. Gregoliński, P. Starynowicz, K. T. Hua, J. L. Lunkley, G. Muller, J. Lisowski, *J. Am. Chem. Soc.* **2008**, *130*, 17761; c) S. D. Bonsall, M. Houcheime, D. A. Straus, G. Muller, *Chem. Commun*. **2007**, 3676.

[15] G. Canard, S. Koeller, G. Bernardinelli, C. Piguet, *J. Am. Chem. Soc.* **2008**, *130*, 1025; T. Riis-Johannessen, N. Dupont, G. Canard, G. Bernardinelli, A. Hauser, C. Piguet, *Dalton Trans.* **2008**, 3661; G. Canard, C. Piguet, *Inorg. Chem*. **2007**, *46*, 3511; N. Dalla-Favera, J. Hamacek, M. Borkovec, D. Jeannerat, G. Ercolani, C. Piguet, *Inorg. Chem*. **2007**, *46*, 9312; M. Albrecht, S. Schmid, S. Dehn, C. Wickleder, S. Zhang, A. P. Bassett, Z. Pikramenou, R. Fröhlich, *New J. Chem*. **2007**, *31*, 1755; J.-M. Senegas, S. Koeller, G. Bernardinelli, C. Piguet, *Chem. Commun*. **2005**, 2235; M. Cantuel, G. Bernardinelli, G. Muller, J. P. Riehl, C. Piguet, *Inorg. Chem*. **2004**, *43*, 1840.

[16] J.-C. G. Bünzli, A.-S. Chauvin, C. D. B. Vandevyver, S. Bo, S. Comby, *Ann. N.Y. Acad. Sci.* **2008**, *1130*, 97; A.-S. Chauvin, S. Comby, B. Song, C. D. B. Vandevyver, F. Thomas, J.-C. G. Bünzli, *Chem.–Eur. J.* **2007**, *13*, 9515; A.-S. Chauvin, S. Comby, B. Song, C. D. B. Vandevyver, J.-C. G. Bünzli, *Chem.–Eur. J.* **2008**, *14*, 1726; B. Song, C. D. B. Vandevyver, A.-S. Chauvin, J.-C. G. Bünzli, *Org. Biomol. Chem.* **2008**, *6*, 4125.

[17] J.-C. G. Bünzli, C. Piguet, *Chem. Soc. Rev*. **2005**, *34*, 1048; J.-C. G. Bünzli, C. Piguet, *Chem. Rev*. **2002**, *102*, 1897.

[18] F. R. Gonçalves e Silva, O. L. Malta, C. Reinhard, H.-U. Güdel, C. Piguet, J. E. Moser, J.-C. G. Bünzli, *J. Phys. Chem. A* **2002**, *106*, 1670; D. Imbert, M. Cantuel, J.-C. G. Bünzli, G. Bernardinelli, C. Piguet, *J. Am. Chem. Soc.* **2003**, *125*, 15698; S. Floquet, N. Ouali, B. Bocquet, G. Bernardinelli, D. Imbert, J.-C. G. Bünzli, G. Hopfgartner, C. Piguet, *Chem.–Eur. J.* **2003**, *9*, 1860; S. Torelli, D. Imbert, M. Cantuel, G. Bernardinelli, S. Delahaye, A. Hauser, J.-C. G. Bünzli, C. Piguet, *Chem.–Eur. J.* **2005**, *11*, 3228; M. Cantuel, F. Gumy, J.-C. G. Bünzli, C. Piguet, *Dalton Trans.* **2006**, 2647.

[19] A. M. Nonat, S. J. Quinn, T. Gunnlaugsson, *Inorg. Chem.* **2009**, *48*, 4646; K. Sénéchal-David, S. J. A. Pope, S. Quinn, S. Faulkner, T. Gunnlaugsson, *Inorg. Chem*. **2006**, *45*, 10040.

[20] S. E. Plush, T. Gunnlaugsson, *Dalton Trans.* **2008**, 3801; S. E. Plush, T. Gunnlaugsson, *Org. Lett*. **2007**, *9*, 1919; K. Sénéshal-David, J. P. Leonard, S. E. Plush, T. Gunnlaugsson, *Org. Lett*. **2006**, *8*, 2727; T. Gunnlaugsson, J. P. Leonard, K. Sénéchal, A. J. Harte, *Chem. Commun.* **2004**, 782.

[21] C. S. Bonnet, T. Gunnlaugsson, *New J. Chem*. **2009**, *33*, 1025; C. M. G. dos Santos, T. Gunnlaugsson, *Supramol. Chem*. **2009**, *21*, 173; C. S. Bonnet, M. Devocelle, T. Gunnlaugsson, *Chem. Commun*. **2008**, 4552.

[22] J. Massue, S. J. Quinn, T. Gunnlaugsson, *J. Am. Chem. Soc.* **2008**, *130*, 6900; J. P. Leonard, C. M. G. dos Santos, S. E. Plush, T. McCabe, T. Gunnlaugsson, *Chem. Commun*. **2007**, 129; A. J. Harte, P. Jensen, S. E. Plush, P. E. Kruger, T. Gunnlaugsson, *Inorg. Chem.* **2006**, *45*, 9465; T. Gunnlaugsson, J. P. Leonard, *Chem. Commun*. **2005**, 3114; T. Gunnlaugsson, J. P. Leonard, *Dalton Trans.* **2005**, 3204; T. Gunnlaugsson, A. J. Harte, J. P. Leonard, M. Nieuwenhuyzen, *Supramol. Chem.* **2003**, *15*, 505.

[23] J. P. Leonard, P. Jensen, T. McCabe, J. E. O'Brien, R. D. Peacock, P. E. Kruger, T. Gunnlaugsson, *J. Am. Chem. Soc.* **2007**, *129*, 10986.

[24] F. Stomeo, C. Lincheneau, J. P. Leonard, J. E. O'Brien, R. D. Peacock, C. P. McCoy, T. Gunnlaugsson, *J. Am. Chem. Soc.* **2009**, *131*, 9636.

[25] Y. Hamuro, S. J. Geib, A. D. Hamilton, *J. Am. Chem. Soc.* **1997**, *119*, 10587.

Received June 4, 2009